# Bifurcations of synchronized responses in synaptically coupled Bonhöffer−van der Pol neurons

Kunichika Tsumoto,[1,*] Tetsuya Yoshinaga,[2,†] and Hiroshi Kawakami[1,‡]

[1]*Department of Electrical and Electronic Engineering, Faculty of Engineering, The University of Tokushima, Tokushima, 770-8506 Japan*

[2]*Department of Radiologic Science and Engineering, School of Health Sciences, The University of Tokushima, Tokushima, 770-8509 Japan*

The Bonhöffer–van der Pol (BvdP) equation is considered as an important model for studying dynamics in a single neuron. In this paper, we investigate bifurcations of periodic solutions in model equations of four and five BvdP neurons coupled through the characteristics of synaptic transmissions with a time delay. The model can be considered as a dynamical system whose solution includes jumps depending on a condition related to the behavior of the trajectory. Although the solution is discontinuous, we can define the Poincaré map as a synthesis of successive submaps, and give its derivatives for obtaining periodic points and their bifurcations. Using our proposed numerical method, we clarify mechanisms of bifurcations among synchronized oscillations with phase-locking patterns by analyzing periodic solutions observed in the coupling system and its subsystems. Moreover, we show that a global behavior of chaotic itinerancy or a phenomenon of chaotic transitions among several quasiattracting states can be observed in higher-dimensional systems of the synaptically four and five coupled neurons.

## I. INTRODUCTION

Synchronization of oscillatory phenomena in globally coupled neuronal models have been investigated extensively to understand information processing in the brain [1,2]. The Bonhöffer–van der Pol (BvdP) or the FitzHugh–Nagumo [3–5] neuron is considered as an important model for studying dynamics in a single neuron. Although there are lots of papers on synchronization phenomena in linearly coupled neuronal oscillators, relatively little has been investigated for a more realistic model describing the time-dependent conductance of the synapse [6–8]. We consider a model of neurons coupled through delayed $\alpha$ functions [9] for describing the characteristics of synaptic transmissions with a time delay.

In Ref. [10], we have formalized the model as a dynamical system whose solution includes jumps depending on a condition related to the behavior of the trajectory; and then we have proposed a numerical method for calculating bifurcations of periodic solutions observed in a coupling system with arbitrary number of Hodgkin-Huxley (HH) neurons [11]. The validity was illustrated using two coupled HH equations. From the analysis, we have clarified mechanisms of transitions of in-phase and antiphase periodic solutions, chaotic oscillations and so on. However, in considering the method for applying to the system with a large number of coupling, the BvdP neuronal model, which is considered as a simplified equation of the four-dimensional HH equation, has an advantage. In Ref. [12], we have shown a parameter set of the BvdP system, such that the two kinds of models with coupling of two and three neurons are qualitatively very

similar in a bifurcational point of view. In this paper, we investigate bifurcations of periodic solutions in model equations of synaptically coupled BvdP neurons with coupling numbers four and five. Because of all-to-all coupling structure having the same coupling coefficients, the system has symmetric properties. We formulate all kinds of subsystems with delayed mutual- and self-coupling and analyze symmetric solutions with phase-locking patterns, which behave in invariant subspaces.

In the four- and five-coupled-neuron systems, we observe a global behavior of the chaotic itinerancy [13–15], which is known as a phenomenon of chaotic transitions among several quasiattracting states, regarded as a model phenomenon for interpreting an associative dynamics or a memory searching process [16,17] in the brain. The bifurcation analysis gives rise to this observation for the Hodgkin-Huxley type neuronal network with synaptic coupling.

## II. COUPLED BvdP EQUATIONS

Let us consider the $N$-coupled BvdP system consisting of the $i$th BvdP equation

$$\frac{dx^{[i]}}{dt} = c\left(x^{[i]} + y^{[i]} - \tfrac{1}{3}x^{[i]^3} + z^{[i]}\right),$$

$$\frac{dy^{[i]}}{dt} = -\frac{1}{c}\left(x^{[i]} + by^{[i]} + a\right), \tag{2.1}$$

and the $i$th linear differential equations

$$\frac{d\alpha^{[i]}}{dt} = \frac{\beta^{[i]}}{\tau},$$

$$\frac{d\beta^{[i]}}{dt} = -2\frac{\beta^{[i]}}{\tau} - \frac{\alpha^{[i]}}{\tau}, \tag{2.2}$$

*Email address: tsu@ee.tokushima-u.ac.jp
†Email address: yosinaga@medsci.tokushima-u.ac.jp
‡Email address: kawakami@ee.tokushima-u.ac.jp
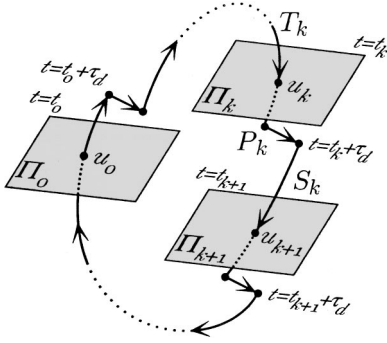
FIG. 1. A schematic diagram of discontinuous trajectory.

for $i=1,2,...,N$. Note that the solution of the variable $\alpha^{[i]}$ in Eq. (2.2) with initial condition $(\alpha^{[i]},\beta^{[i]})=(0,1)$ at $t=0$ represents the $\alpha$ function [9] or $\alpha^{[i]}(t)=(t/\tau)e^{-t/\tau}$, which is a model for describing the time-dependent conductance of the synapse. In Eq. (2.1), the following definition is used:

$$z^{[i]}=-\sum_{j\neq i}\frac{d}{N-1}(x^{[i]}-\hat{x})\alpha^{[j]}, \qquad (2.3)$$

where $\hat{x}$ represents the synaptic reversal potential [9], which depends on the type of synaptic transmitter released from a presynaptic neuron and their receptors. The coupling becomes excitatory and inhibitory with $\hat{x}>x_{eq}$ and $\hat{x}<x_{eq}$, respectively, where $x_{eq}$ denotes an equilibrium potential of every neuron.

We assume that a firing of the membrane potential of the $i$th neuron occurs when the state variable $x^{[i]}$ crosses zero as a threshold value with changing its sign from negative to positive. Each vector $(\alpha^{[i]},\beta^{[i]})$ jumps to the constant $(0,1)$ at $t=t_0^{[i]}+\tau_d$ where $t_0^{[i]}$ is the time when $x^{[i]}$ changes to $x^{[i]}>0$. Namely, the firing information of a neuron transforms to all other neurons with the time delay $\tau_d$.

### III. METHOD OF ANALYSIS

We summarize methods for calculating bifurcations in a class of dynamical systems including the coupled BvdP equations defined in the preceding section. We treat the system such that its solution jumps to a constant value at $\tau_d$ past the time when the solution crosses one of several local sections in the state space.

Consider a set of general autonomous differential equations consisting of Eqs. (2.1) and (2.2), for $i=1,2,...,N$, such that

$$\frac{dX}{dt}=f(X), \qquad (3.1)$$

where $X$ is the state $X=(x^{[1]},y^{[1]},\alpha^{[1]},\beta^{[1]},...,x^{[N]},y^{[N]},\alpha^{[N]},\beta^{[N]})'\in R^n$ with $n=4N$, where $(\ )'$ denotes the transpose. We assume that there exists a solution with initial condition $X=X_0$ at $t=t_0$, denoted by $X(t)=\varphi(t;t_0,X_0)$, for all $t$.

### A. Poincaré map

Figure 1 shows a schematic diagram of a discontinuous trajectory with jumps in the state space. A local section $M_k$ of the subspace $\Pi_k$ in Fig. 1 and its local coordinate $h_k$ for $k=0,1,...,m-1$ are, respectively, denoted by

$$M_k=\{X\in R^n:g_k(X)=0,g_k:R^n\to R\}$$

$$h_k:M_k\to\Pi_k\subset R^{n-1};X_k\mapsto u_k. \qquad (3.2)$$

Then, the Poincaré map

$$T:\Pi_0\to\Pi_0;\quad u_0\mapsto T(u_0), \qquad (3.3)$$

can be defined by $T=T_m$, where $T_m$ is given by the following successive formula for $k=0,1,...,m-1$:

$$T_{k+1}(u_0)=S_k\circ T_k(u_0), \qquad (3.4)$$

with $T_0$ as the identical map. The map $S_k$ in Eq. (3.4) is given by

$$S_k:\Pi_k\to\Pi_{k+1}$$

$$u_k\mapsto h_{k+1}\circ\varphi(\tau_k(h_k^{-1}(u_k))+t_k:\tau_d+t_k,$$

$$P_k\circ\varphi(\tau_d+t_k;t_k,h_k^{-1}(u_k))), \qquad (3.5)$$

where $\tau_k(h_k^{-1}(u_k))$ is the time in which the trajectory emanating from a point $h_k^{-1}(u_k)$ on the local section $M_k$ at $t=t_k$ will hit the next local section $M_{k+1}$. Moreover, $P_k$ is the map such that a set of the elements in $X_k\in R^n$: $\{(\alpha_k^{[j]},\beta_k^{[j]}):j\in J_k\}$, for some $J_k\subset[1,2,...,N]$, is mapped to the constant vector $(0,1)$, i.e.,

$$P_k:R^n\to R^n$$

$$X_k\mapsto(x_k^{[1]},y_k^{[1]},\alpha_k^{[1]},\beta_k^{[1]},...,x_k^{[j]},y_k^{[j]},0,1,...,x_k^{[N]},$$

$$y_k^{[N]},\alpha_k^{[N]},\beta_k^{[N]})'$$

$$\text{for any }j\in J_k. \qquad (3.6)$$

For calculating bifurcation sets of a fixed point observed in the Poincaré map $T$, it is required to obtain the first and the second derivatives with respect to the initial state and/or the system parameter.

The first derivative of $T$ with respect to the initial state $u_0$, or

$$\frac{\partial T}{\partial u_0}=\frac{\partial T_m}{\partial u_0},$$

is given by obtaining the derivatives of the submaps, successively, for $k=0,1,...,m-1$,

$$\frac{\partial T_{k+1}}{\partial u_0}=\frac{\partial S_k}{\partial u_k}\frac{\partial T_k}{\partial u_0}\quad\text{with }\frac{\partial T_0}{\partial u_0}=I, \qquad (3.7)$$

where the derivatives of $S_k$'s are obtained by solving the first-order variational equations, see Appendix.

Moreover, the first and the second derivatives of $T$ with respect to the parameter $\lambda$ and the initial states $u_0$ and $v_0$,

$$\frac{\partial T}{\partial \lambda} = \frac{\partial T_m}{\partial \lambda}, \quad \frac{\partial^2 T}{\partial u_0 \partial v_0} = \frac{\partial^2 T_m}{\partial u_0 \partial v_0}, \quad \frac{\partial^2 T}{\partial u_0 \partial \lambda} = \frac{\partial^2 T_m}{\partial u_0 \partial \lambda},$$

are given by obtaining the derivatives of the submaps, successively, for $k = 0, 1, ..., m-1$,

$$\frac{\partial T_{k+1}}{\partial \lambda} = \frac{\partial S_k}{\partial \lambda} + \frac{\partial S_k}{\partial u_k} \frac{\partial T_k}{\partial \lambda},$$

$$\frac{\partial^2 T_{k+1}}{\partial u_0 \partial v_0} = \frac{\partial^2 S_k}{\partial u_k \partial v_k} \frac{\partial T_k}{\partial v_0} \frac{\partial T_k}{\partial u_0} + \frac{\partial S_k}{\partial u_k} \frac{\partial^2 T_k}{\partial u_0 \partial v_0},$$

$$\frac{\partial T_{k+1}}{\partial u_0 \partial \lambda} = \frac{\partial^2 S_k}{\partial u_k \partial \lambda} \frac{\partial T_k}{\partial u_0} + \frac{\partial S_k}{\partial u_k} \frac{\partial^2 T_k}{\partial u_0 \partial \lambda} + \frac{\partial^2 S_k}{\partial u_k \partial v_k} \frac{\partial T_k}{\partial u_0} \frac{\partial T_k}{\partial \lambda}, \quad (3.8)$$

with

$$\frac{\partial T_0}{\partial u_0} = I, \quad \frac{\partial T_0}{\partial \lambda} = 0, \quad \frac{\partial^2 T_0}{\partial u_0 \partial v_0} = 0, \quad \frac{\partial^2 T_0}{\partial u_0 \partial \lambda} = 0.$$

The derivatives of $S_k$'s in Eq. (3.8) are obtained by solving the first- and the second-order variational equations.

### B. Bifurcation of a periodic solution

If a solution of the coupled BvdP system is periodic, then the point $u$ satisfying

$$u - T(u) = 0 \quad (3.9)$$

becomes a fixed point of $T$. Hence the study of a periodic solution observed in the coupled BvdP system is topologically equivalent to the study of a fixed point satisfying Eq. (3.9). Note that an $m$-periodic point can be studied by replacing $T$ with $T^m$, $m$th iterates of $T$, in Eq. (3.9). Therefore, in the following we consider only properties of a fixed point of $T$ and its bifurcations. Similar argument can be applied to the periodic point of $T$.

Let $u \in \Pi_0$ be a fixed point of $T$. Then the characteristic equation of the fixed point $u$ is defined by

$$\det\left( \mu I - \frac{\partial T}{\partial u_0}(u) \right) = 0, \quad (3.10)$$

where $I$ is the $(n-1) \times (n-1)$ identity matrix, and $\partial T(u)/\partial u_0$ denotes the derivative of $T(u)$ with respect to the initial state $u_0$. We call $u$ hyperbolic if all absolute values of the eigenvalues of $\partial T(u)/\partial u_0$ are different from unity. The topological type of a hyperbolic fixed point is determined by the dim$E^u$ and det $L^u$, where $E^u$ is the intersection of $\Pi_0$ and the direct sum of the generalized eigenspaces of $\partial T(u)/\partial u_0$ corresponding to the eigenvalues $\mu$ such that $|\mu| > 1$ and $L^u = \partial T(u)/\partial u_0|_{E^u}$.

A hyperbolic fixed point is called $D$ type, if det $L^u > 0$, and $I$ type if det $L^u < 0$. By this definition we have $2(n-1)$ topologically different types of hyperbolic fixed points. These types are

$$_kD \quad (k = 0, 1, ..., n-1), \quad _kI \quad (k = 1, ..., n-2),$$

where $D$ and $I$ denote the type of the fixed point and the subscript integer indicates the dimension of the unstable subspace: $k = \dim E^u$. This classification is also obtained from the distribution of characteristic multipliers of Eq. (3.10). That is, $D$ and $I$ correspond to the even and odd number of characteristic multipliers on the real axis $(-\infty, -1)$, and $k$ indicates the number of characteristic multiplier outside the unit circle in the complex plane.

Bifurcation occurs when the topological type of a fixed point is changed by the variation of a system parameter. The codimension-one bifurcations that the coupled BvdP system has a possibility to occur are: tangent bifurcation, period-doubling bifurcation, the Neimark-Sacker bifurcation, and $D$ type of branching. These bifurcations are observed when the hyperbolicity is destroyed. The conditions for the former three bifurcations correspond to the critical distribution of the characteristic multiplier: $\mu = +1$, $\mu = -1$, and $|\mu| = 1$, respectively. While, a $D$ type of branching or a pitchfork bifurcation appears in the system that possess some symmetric property. This type of bifurcation occurs when a real characteristic multiplier passes through the point $(1, 0)$ in the complex plane. Thus the bifurcation condition is a degenerate case of the tangent bifurcation.

The numerical determination of the bifurcation set is accomplished by solving the system of equations that represent the relation of fixed point, i.e., Eq. (3.9), and the bifurcation condition, i.e., Eq. (3.10) with the corresponding value of $\mu$. For this purpose, Newton's method is used. The principle idea of this procedure for finding bifurcation parameters was presented by Kawakami [18]. The Jacobian matrix of the set of equations is derived from the derivatives of the map $T$, given in the preceding subsection.

### C. Symmetrical properties

In this subsection, we summarize notations on symmetric properties of the system in Eq. (3.1). A symmetric property of the state space for Eq. (3.1) is defined by the invariance of $f$ under the action of a group $G$, i.e.,

$$gf(X) = f(gX), \quad \forall \ g \in G. \quad (3.11)$$

Then, the function $f$ satisfying Eq. (3.11) is said to be $G$ equivariant [19,20]. The orbit of the action of $G$ on $X \in R^n$ is the set

$$G_X = \{gX : g \in G\}. \quad (3.12)$$

The group $G_X$ is called a $G$ orbit of $X$.

The isotropy subgroup $\Sigma_X$ of $X$ is defined by

$$\Sigma_X = \{g \in G : gX = X\}. \quad (3.13)$$

The elements of the isotropy subgroup of $X$ are called the stabilizers of $X$. We point out that a subgroup of $G$ may not be an isotropy subgroup. The isotropy subgroup defines the symmetry of a point $X$ in the state space. Two points on the same $G$ orbit have conjugate isotropy subgroups, $\Sigma_{gX} = g^{-1}\Sigma_X g$. Two different elements of points have conjugate isotropy subgroups. Its $G$ equivariant forces $f$ to have invari-

ant linear subspaces corresponding to certain subgroups of $G$. The fixed point subspace of a subgroup $H$ of $G$ is defined by

$$S_{\text{fix}}(H) = \{X \in R^n | hX = X, \quad \forall h \in H\}. \quad (3.14)$$

The subspace $S_{\text{fix}}(H)$ is always a linear subspace of $R^n$ since

$$S_{\text{fix}}(H) = \bigcap_{h \in H} \ker(h - I_n), \quad (3.15)$$

where $I_n$ is the $n \times n$ identity matrix.

## IV. ANALYSIS OF SYMMETRY

In this section, we consider symmetric properties depending on the symmetry of the invariant subspace in the state space of four- and five-coupled-neuron systems.

Before considering concrete systems, let us define a phase difference of a periodic solution. We assume a periodic solution of Eq. (3.1) with initial condition $X_0 := X(0)$ exists:

$$X(t) = \varphi(t; 0, X_0). \quad (4.1)$$

If there exists a matrix $g$ and a time $T_0$ such that

$$g \varphi(t; 0, X_0) = \varphi(t; 0, gX_0) = \varphi(t + T_0; 0, X_0), \quad (4.2)$$

for all $t$, then we call it a $(g, T_0)$-symmetric periodic solution. Note that the symmetric periodic solution has two kinds of symmetries, i.e., spatial and temporal symmetries. The temporal symmetry involves a phase difference of wave forms among neurons.

### A. Four coupled neurons

We first consider the system of four coupled BvdP neurons. Equation (3.1) with $N = 4$ is invariant under the possible permutations of the state variables, forming a symmetric group. The matrices constituting the symmetric group are as follows:

$$g_1 = \begin{bmatrix} I_4 & 0 & 0 & 0 \\ 0 & I_4 & 0 & 0 \\ 0 & 0 & I_4 & 0 \\ 0 & 0 & 0 & I_4 \end{bmatrix}, \quad g_2 = \begin{bmatrix} 0 & I_4 & 0 & 0 \\ 0 & 0 & I_4 & 0 \\ 0 & 0 & 0 & I_4 \\ I_4 & 0 & 0 & 0 \end{bmatrix},$$

$$g_3 = \begin{bmatrix} I_4 & 0 & 0 & 0 \\ 0 & 0 & I_4 & 0 \\ 0 & 0 & 0 & I_4 \\ 0 & I_4 & 0 & 0 \end{bmatrix}, \quad g_4 = \begin{bmatrix} I_4 & 0 & 0 & 0 \\ 0 & I_4 & 0 & 0 \\ 0 & 0 & 0 & I_4 \\ 0 & 0 & I_4 & 0 \end{bmatrix},$$

$$g_5 = \begin{bmatrix} 0 & I_4 & 0 & 0 \\ I_4 & 0 & 0 & 0 \\ 0 & 0 & 0 & I_4 \\ 0 & 0 & I_4 & 0 \end{bmatrix},$$



(a) $S_{\text{fix}}(\Sigma_{41})$

(b) $S_{\text{fix}}(\Sigma_{42})$    (c) $S_{\text{fix}}(\Sigma_{43})$    (d) $S_{\text{fix}}(\Sigma_{44})$
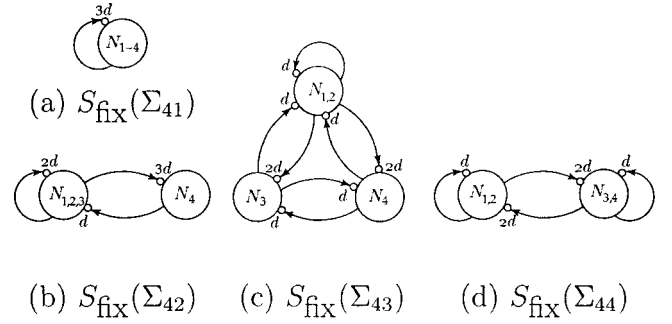
FIG. 2. Schematic diagrams of subsystems with delayed mutual- and self-coupling in the four coupled neurons. In the diagram, $N_i$ denotes the $i$th BvdP neuron for $i = 1,2,3,4$. The coupling coefficient is denoted beside the arrow head indicating the direction of coupling.

The symmetric group has five isotropy subgroups $\Sigma_{41} = \{g_1, g_2, g_2^2, g_2^3\}$, $\Sigma_{42} = \{g_1, g_3, g_3^2\}$, $\Sigma_{43} = \{g_1, g_4\}$, $\Sigma_{44} = \{g_1, g_5\}$, and $\Sigma_{45} = \{g_1\}$. We can define invariant subspaces as follows:

$$S_{\text{fix}}(\Sigma_{41}) = \{[X_a' \ X_a' \ X_a' \ X_a']' \in R^{16} | X_a \in R^4\},$$

$$S_{\text{fix}}(\Sigma_{42}) = \{[X_a' X_b' \ X_b' \ X_b']' \in R^{16} | X_a, \ X_b \in R^4\},$$

$$S_{\text{fix}}(\Sigma_{43}) = \{[X_a' \ X_b' \ X_c' \ X_c']' \in R^{16} | X_a, X_b, X_c \in R^4\},$$

$$S_{\text{fix}}(\Sigma_{44}) = \{[X_a' \ X_a' \ X_b' \ X_b']' \in R^{16} | X_a, X_b \in R^4\},$$

We note that the behavior of a symmetric periodic solution with a phase-locking pattern is restricted to an invariant subspace. One of analyses for phase-locked periodic solutions can be reduced to an analysis for periodic solutions observed in simplified systems with delayed mutual- and self-coupling, as shown in Fig. 2. For example, an entirely in-phase and an antiphase periodic solutions, which are possibly observed in the system, appear in $S_{\text{fix}}(\Sigma_{41})$ and $S_{\text{fix}}(\Sigma_{44})$, respectively. The antiphase response is a $(g_2^2, L/2)$-symmetric periodic solution, where $L$ is the period of the periodic solution.

### B. Five coupled neurons

Next, we consider the system of five coupled BvdP neurons. The function $f$ in Eq. (3.1) with $N = 5$ is commutative with respect to an element of the symmetric group. According to the similar discussion of symmetric properties in the previous coupling case, we obtain simplified systems for the analysis of entirely and partially in-phase periodic solutions, as shown in Fig. 3, which behave in the following invariant subspaces:

$$S_{\text{fix}}(\Sigma_{51}) = \{[X_a' \ X_a' \ X_a' \ X_a' \ X_a']' \in R^{20} | X_a \in R^4\},$$

(a) $S_{\text{fix}}(\Sigma_{51})$     (b) $S_{\text{fix}}(\Sigma_{52})$     (c) $S_{\text{fix}}(\Sigma_{53})$



(d) $S_{\text{fix}}(\Sigma_{54})$     (e) $S_{\text{fix}}(\Sigma_{55})$     (f) $S_{\text{fix}}(\Sigma_{56})$
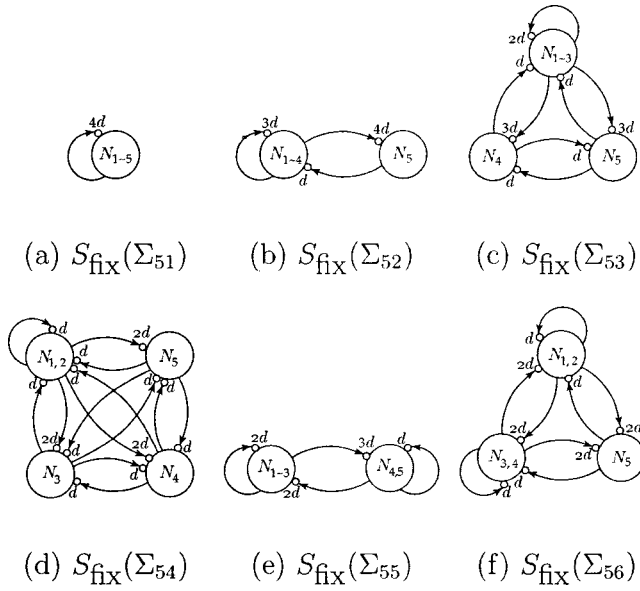
FIG. 3. Schematic diagrams of subsystems with delayed mutual- and self-coupling in the five coupled neurons. In the diagram, $N_i$ denotes the $i$th BvdP neuron for $i=1,2,\ldots,5$.

$$S_{\text{fix}}(\Sigma_{52})=\{[X'_a\ X'_b\ X'_b\ X'_b\ X'_b]'\in R^{20}|X_a,X_b\in R^4\},$$

$$S_{\text{fix}}(\Sigma_{53})=\{[X'_a\ X'_b\ X'_c\ X'_c\ X'_c]'\in R^{20}|X_a,X_b,X_c\in R^4\},$$

$$S_{\text{fix}}(\Sigma_{54})=\{[X'_a\ X'_b\ X'_c\ X'_d\ X'_d]'$$
$$\in R^{20}|X_a,X_b,X_c,X_d\in R^4\},$$

$$S_{\text{fix}}(\Sigma_{55})=\{[X'_a\ X'_a\ X'_b X'_b\ X'_b]'\in R^{20}|X_a,X_b\in R^4\},$$

$$S_{\text{fix}}(\Sigma_{56})=\{[X'_a\ X'_b\ X'_b X'_c\ X'_c]'\in R^{20}|X_a,X_b,X_c\in R^4\}.$$

## V. ANALYSIS OF BIFURCATION

This section is devoted to showing numerical results obtained from bifurcation analysis of four- and five-coupled-BvdP-neuron systems. In order to view results of two- and three-coupled-BvdP-neuron systems, see Ref. [12].

In the following, we fix several system parameters in Eqs. (2.1)–(2.3) as $a=0.3$, $b=0.8$, $c=3$, $\tau=2$, and $\hat{x}=-0.3$, and change the values of the coupling coefficient $d$ and the time delay $\tau_d$. We remark that the following results were calculated by the fourth-order Runge-Kutta method with the double precision numbers. We used the method of bisection for detecting threshold crossing and checked if both property of solutions and global structure of bifurcation diagrams did not change qualitatively, due to the variation of the tolerance of the bisection as well as the step size of numerical integration.

Before showing results, we summarize some notations. The symbols $_kD_l^m$ and $_kI_l^m$ denote hyperbolic periodic points, where $k$ indicates the number of characteristic multiplier out-
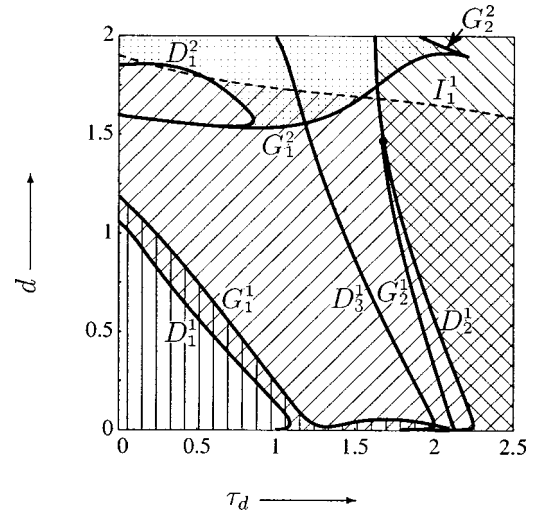


FIG. 4. Bifurcation diagram for periodic solutions in four coupled BvdP neurons.

side the unit circle in the complex plane, $m$ indicates $m$-periodic point, and $l$ indicates the number to distinguish the several same sets, if necessary. In the bifurcation diagram, we use notations: $G_l^m$, $I_l^m$, $N_l^m$, and $D_l^m$ for tangent bifurcation, period-doubling bifurcation, the Neimark–Sacker bifurcation, and $D$ type of branching, respectively, where $m$ indicates a bifurcation set for $m$-periodic point and $l$ indicates the number to distinguish the several same sets, if they exist.

### A. Bifurcations in four coupled BvdP neurons

We consider a system of four coupled BvdP neurons. By analyzing periodic solutions observed in several subsystems as shown in Fig. 2, we obtained a bifurcation diagram for periodic solutions, see Fig. 4. In this figure, the shaded portions denote parameters at which various types of stable periodic solutions exist: backward diagonal (///) for an entirely in-phase solution in $S_{\text{fix}}(\Sigma_{41})$, vertical (|||) for a partially in-phase solution in $S_{\text{fix}}(\Sigma_{42})$, forward diagonal (\\\\) for an antiphase solution in $S_{\text{fix}}(\Sigma_{44})$, and dotted portion for a two-periodic solution in $S_{\text{fix}}(\Sigma_{44})$. The regions overlapped by several patterns denote coexistence of the corresponding solutions, depending on the initial condition. Examples of various kinds of attractors with phase-locking patterns are shown in Fig. 5.

When the value of $\tau_d$ increases across the bifurcation set $D_2^1$ in Fig. 4, we observe the $D$ type of branching with formula

$$_1D_1^1+2\ _0D_2^1\to\ _0D_1^1,$$

where the left- and right-hand sides of the arrow indicate the periodic points before and after the bifurcation, respectively. This bifurcation formula represents a transition between a partially in-phase ($_0D_2^1$) and an antiphase ($_0D_1^1$) periodic solutions as shown in Figs. 5(d) and (e), respectively. On the other hand, the $D$ type of branching $D_3^1$ causes a bifurcation between unstable partially in-phase periodic solutions in $S_{\text{fix}}(\Sigma_{44})$ and in $S_{\text{fix}}(\Sigma_{43})$.

(a) entirely in-phase

solution in $S_{\text{fix}}(\Sigma_{41})$

$(\tau_d = 1, d = 0.9)$

(b) partially in-phase

solution in $S_{\text{fix}}(\Sigma_{42})$

$(\tau_d = 0.5, d = 0.3)$

(c) partially in-phase

solution in $S_{\text{fix}}(\Sigma_{43})$

$(\tau_d = 1.844819, d = 0.9)$

(d) partially in-phase

solution in $S_{\text{fix}}(\Sigma_{44})$

$(\tau_d = 1.85, d = 0.9)$

(e) anti-phase

solution in $S_{\text{fix}}(\Sigma_{44})$

$(\tau_d = 2.3, d = 0.9)$

(f) 2-periodic solution

in $S_{\text{fix}}(\Sigma_{44})$

$(\tau_d = 1, d = 1.95)$
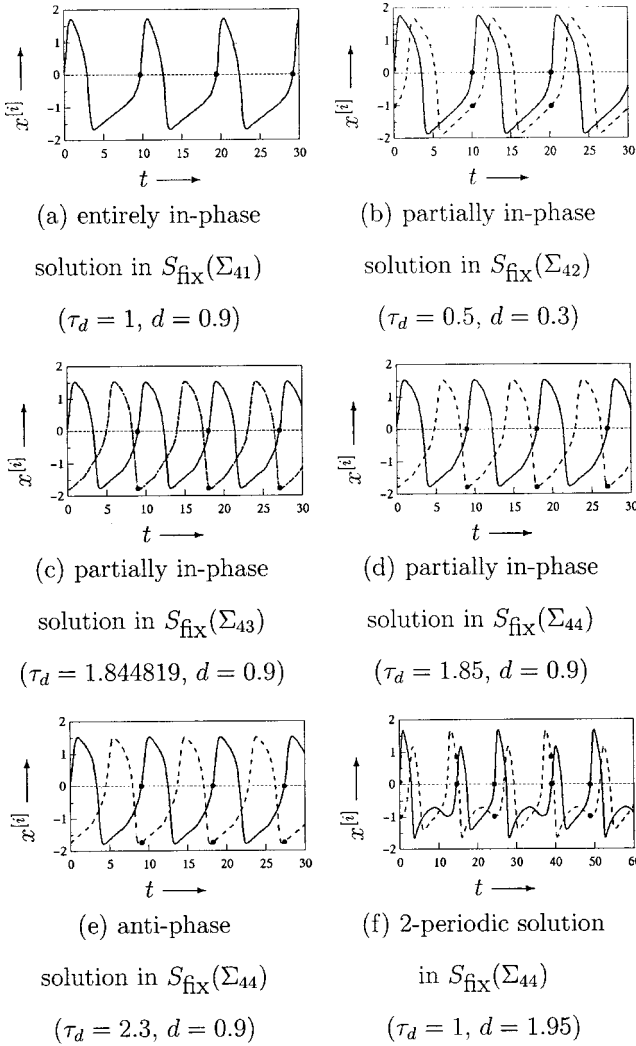
FIG. 5. Examples of periodic solutions observed in four coupled neurons. The circled points denote iterated points by Poincaré map.

## B. Bifurcations in five coupled BvdP neurons

Next, we consider a system of five coupled BvdP neurons. Figure 6 shows a bifurcation diagram obtained from the analysis of periodic solutions observed in several subsystems as shown in Fig. 3. The parameter regions at which stable periodic solutions exist are marked by the shading: backward diagonal (///) for an entirely in-phase solution in $S_{\text{fix}}(\Sigma_{51})$, vertical (|||) for a partially in-phase solution in $S_{\text{fix}}(\Sigma_{52})$, forward diagonal (\\\\) for a partially in-phase solution in $S_{\text{fix}}(\Sigma_{55})$, dark shaded portion for a nearly triphase solution in $S_{\text{fix}}(\Sigma_{56})$, and dotted protion for a two-periodic solution in $S_{\text{fix}}(\Sigma_{55})$. Examples of various kinds of attractors with phase-locking patterns are shown in Fig. 7.

When the value of $\tau_d$ increases across the bifurcation set $D_2^1$ in Fig. 6, we observe the $D$ type of branching with formula:

$$_1D_1^1 \rightarrow {}_0D_1^1 + 2\ {}_1D_2^1,$$

where $_1D_2^1$ is an unstable partially in-phase periodic solution
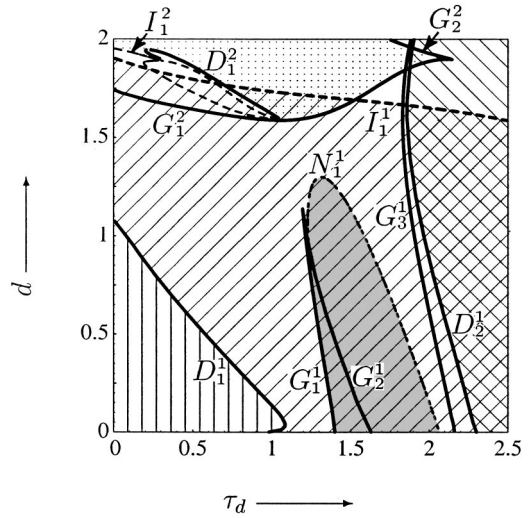


FIG. 6. Bifurcation diagram for periodic solutions in five coupled BvdP neurons.



(a) entirely in-phase

solution in $S_{\text{fix}}(\Sigma_{51})$

$(\tau_d = 1, d = 1.2)$

(b) partially in-phase

solution in $S_{\text{fix}}(\Sigma_{52})$

$(\tau_d = 0.5, d = 0.4)$

(c) partially in-phase

solution in $S_{\text{fix}}(\Sigma_{55})$

$(\tau_d = 2.3, d = 1.2)$

(d) partially in-phase

solution in $S_{\text{fix}}(\Sigma_{56})$

$(\tau_d = 1.5, d = 0.8)$

(e) 2-periodic solution

in $S_{\text{fix}}(\Sigma_{55})$

$(\tau_d = 1.0, d = 1.8)$

(f) chaotic oscillation

in $S_{\text{fix}}(\Sigma_{55})$

$(\tau_d = 1.75, d = 1.76)$
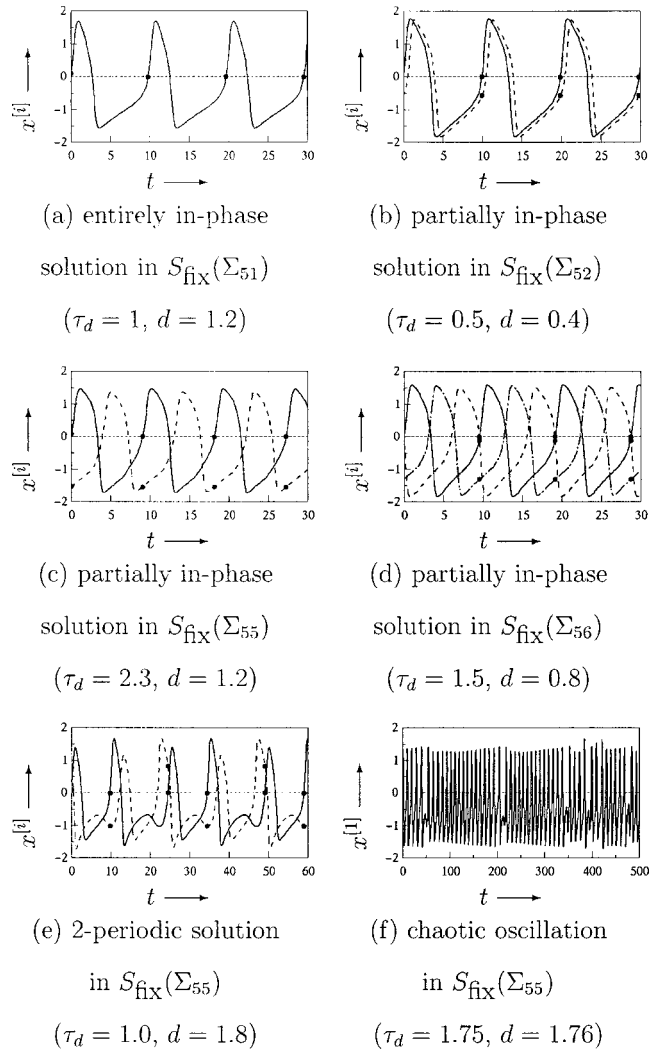
FIG. 7. Examples of attractors observed in five coupled neurons. The circled points denote iterated points by Poincaré map.

(a) $x^{[1]} - x^{[2]}$



(b) $x^{[3]} - x^{[4]}$



(c) $x^{[2]} - x^{[3]}$



(d) $x^{[4]} - x^{[1]}$
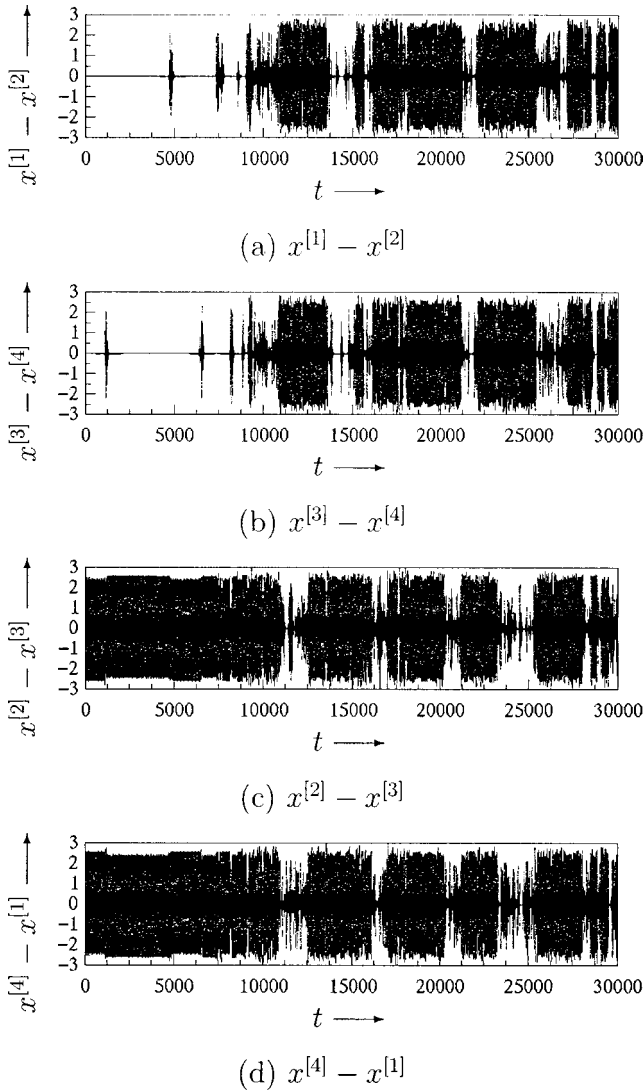
FIG. 8. A chaotic itinerary observed in the four-coupled-neuron system at $(\tau_d, d) = (0.35, 1.8036)$.

in $S_{\text{fix}}(\Sigma_{53})$. In the triangle region without shading in Fig. 6, we observe chaotic attractors which behave in various kinds of invariant subspaces, see Fig. 7 for an example of chaos in $S_{\text{fix}}(\Sigma_{55})$.

### C. Global behavior of chaotic attractor

In this subsection, to illustrate differences on dynamics between low- and high-dimensional coupled systems, we show a global behavior observed in the high-dimensional systems of four- and five coupled BvdP neurons.

Figure 8 shows wave forms of a chaotic attractor in the four-coupled-neuron system. The attractor exhibits a temporal partial synchronization with switching clusters: one in which both $|x^{[1]} - x^{[2]}|$ and $|x^{[3]} - x^{[4]}|$ are small, and another in which both $|x^{[2]} - x^{[3]}|$ and $|x^{[4]} - x^{[1]}|$ are small. Recall that the state space includes the invariant subspace $S_{\text{fix}}(\Sigma_{44})$ and its conjugate subspaces. Therefore, this phenomenon is considered as a chaotic itinerary among several
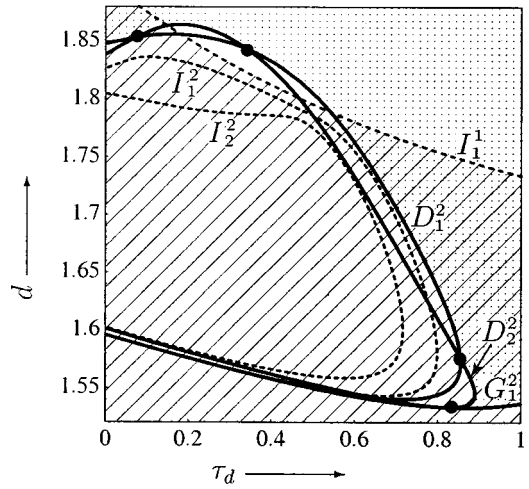


FIG. 9. Enlarged bifurcation diagram of Fig. 4.

quasiattracting states in the neighborhoods of invariant subspaces.

The parameter at which the chaos can be seen is determined as follows. Figure 9 shows an enlarged bifurcation diagram of Fig. 4. To see the relation among bifurcation sets and the property of periodic points, we show a schematic one-parameter bifurcation diagram with variation of the parameter $d$ for fixed $\tau_d = 0.5$, in Fig. 10. In the figure, $_0D_1^2$ indicates a two-periodic solution restricted in the invariant subspace $S_{\text{fix}}(\Sigma_{44})$. By decreasing the value of $d$ continuously, a couple of stable asymmetric two-periodic solutions $_0D_2^2$ caused by the $D$ type of branching of $_0D_1^2$ bifurcates to $_1D_2^2$ and $_2I_2^2$ through the bifurcations $D_3^2$ and $I_1^2$, respectively. We have a cascade of period-doubling bifurcations toward chaotic itinerary, by further decreasing of $d$. The parameter range in which the chaos can be seen is very small and additionally the attractor coexists with a stable periodic solution as shown in Fig. 9. Hence we assert that bifurcation analysis of periodic solutions is very useful for detecting chaotic attractor.

Similar phenomenon of global chaotic behavior can be observed for the five-coupled-neuron system, see Fig. 11 for an example. From this figure, the quasiattracting states that
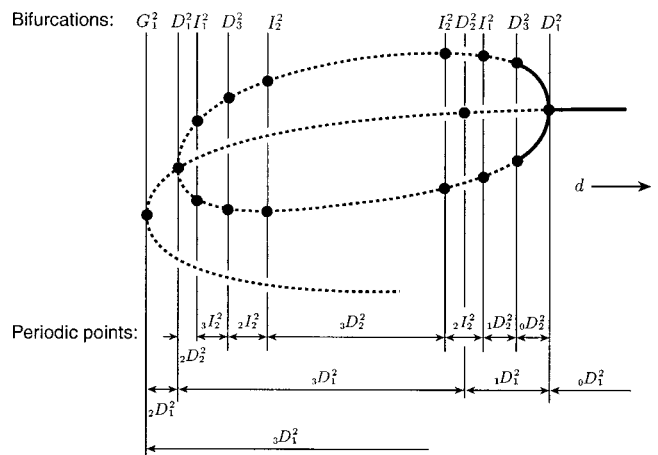


FIG. 10. A schematic diagram of one-parameter bifurcations.

(a) $x^{[2]} - x^{[3]}$



(b) $x^{[5]} - x^{[2]}$



(c) $x^{[4]} - x^{[5]}$



(d) $x^{[5]} - x^{[1]}$
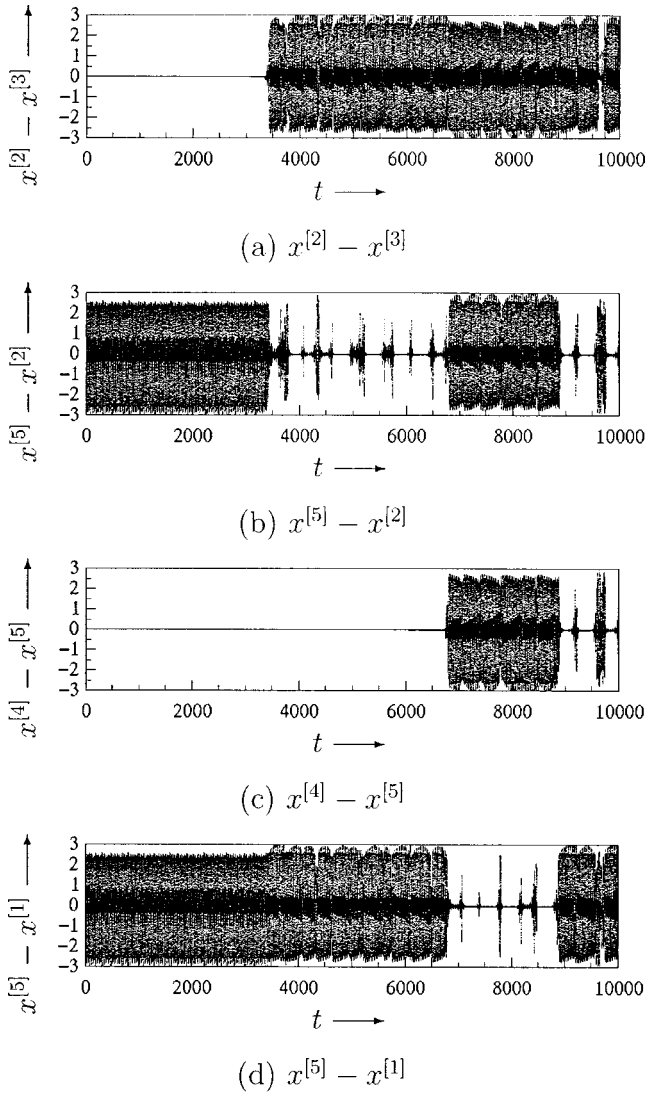
FIG. 11. A chaotic itinerancy observed in the five-coupled-neuron system at $(\tau_d, d) = (0.585, 1.8)$.

the trajectory itinerants are near subspaces satisfying $x^{[1]} = x^{[2]} = x^{[3]}$ and $x^{[4]} = x^{[5]}$ for $t$ in around $[0, 3400]$; $x^{[1]} = x^{[3]}$ and $x^{[2]} = x^{[4]} = x^{[5]}$ for $t$ in around $[3400, 6800]$; $x^{[1]} = x^{[3]} = x^{[5]}$ and $x^{[2]} = x^{[4]}$ for $t$ in around $[6800, 8900]$ and so on.

## VI. CONCLUDING REMARKS

We have investigated mechanisms of various bifurcation phenomena observed in BvdP neurons coupled through the characteristics of synaptic transmissions with a time delay. The main results obtained from the analysis are summarized as follows

(1) We formulated all kinds of subsystems with delayed mutual-and self-coupling and analyzed symmetric solutions with phase-locking patterns, which behave in invariant subspaces.

(2) We calculated bifurcations of periodic solutions with various kinds of synchronization. We found mechanisms of

transitions among not only various types of periodic solutions but also chaotic oscillations.

(3) Chaotic attractor appearing in this paper is essentially caused by the effect of coupling. This is easily understood by the fact that the single BvdP equation cannot generate a chaos.

(4) Moreover, we have shown a phenomenon of chaotic itinerancy for both four and five coupled neurons. It is conjectured that the four-coupled-neuron system, which is considered as a mutual coupling system of two chaotic neurons in certain parameter setting, is the minimal system generating a chaotic itinerancy. We note that the bifurcation analysis plays an essential role for finding this type of global chaotic attractor, because the chaos can be seen in a very small parameter region and coexists with a stable periodic solution.

The synaptically coupled BvdP model with rich global dynamics is adequate to reproduce various types of synchronized oscillations in a neuronal network. Further analyses are needed for clarifying a mechanism of the generation of global chaotic behavior.

## APPENDIX: THE DERIVATIVES OF SUBMAPS

From the definition of $S_k$ in Eq. (3.5), the derivative of $S_k$ with respect to the initial state $u_k$ is given by

$$
\begin{aligned}
\frac{\partial S_k}{\partial u_k} &= \frac{\partial h_{k+1}}{\partial x_{k+1}} \left( \frac{\partial \varphi}{\partial x_k}(\tau_k + t_k; t_k, x_k) \right. \\
&\quad + f(h_{k+1}^{-1}(u_{k+1})) \frac{\partial \tau_k}{\partial x_k} \right) \frac{\partial h_k^{-1}}{\partial u_k} \\
&= \frac{\partial h_{k+1}}{\partial x_{k+1}} \left( I - \frac{1}{\dfrac{\partial g_{k+1}}{\partial x_{k+1}} f(h_{k+1}^{-1}(u_{k+1}))} \right. \\
&\quad \left. \times f(h_{k+1}^{-1}(u_{k+1})) \frac{\partial g_{k+1}}{\partial x_{k+1}} \right) \frac{\partial \varphi}{\partial x_k}(\tau_k + t_k; t_k, x_k) \frac{\partial h_k^{-1}}{\partial u_k},
\end{aligned}
$$

(A1)

where the second equation is obtained by eliminating $\partial \tau_k / \partial x_k$ in the first equation, which comes from the relation

$$
\frac{\partial}{\partial x_k} g_{k+1}[\varphi(\tau_k(x_k) + t_k; t_k, x_k)] = 0,
$$

since $x_{k+1} = \varphi(\tau_k(x_k) + t_k; t_k, x_k) \in M_{k+1}$ holds for any $x_k \in M_k$. Note that, in Eq. (A1), the transversability of the solution with respect to $M_{k+1}$ guarantees

$$
\frac{\partial g_{k+1}}{\partial x_{k+1}} f(h_{k+1}^{-1}(u_{k+1})) \neq 0.
$$

On the other hand, to avoid the discontinuity of the solution at $t = \tau_d + t_k$, we have

$$\frac{\partial \varphi}{\partial x_k}(\tau_k + t_k ; t_k, x_k)$$

$$= \frac{\partial \varphi}{\partial y_k}(g t_k + t_k ; \tau_d + t_k, y_k)\frac{\partial \varphi}{\partial x_k}(\tau_d + t_k ; t_k, x_k).$$

The right-hand side of the above equation is obtained by solving the first-order variational equations:

$$\frac{d}{dt}\frac{\partial \varphi}{\partial x_k} = \frac{\partial f}{\partial x}\frac{\partial \varphi}{\partial x_k} \quad \text{with} \quad \left.\frac{\partial \varphi}{\partial x_k}\right|_{t=t_k} = I, \qquad (A2)$$

$$\frac{d}{dt}\frac{\partial \varphi}{\partial y_k} = \frac{\partial f}{\partial x}\frac{\partial \varphi}{\partial y_k} \quad \text{with} \quad \left.\frac{\partial \varphi}{\partial y_k}\right|_{t=\tau_d+t_k} = I, \qquad (A3)$$

and putting $t = \tau_d + t_k$ and $\tau_k + t_k$ in the solutions of Eqs. (A2) and (A3), respectively. The derivation of the first and the second derivatives of $S_k$ with respect to $\lambda$, $u_k$ and $v_k$, in Eq. (3.8) is similar.

[1] H. Golomb, D. Hansel, B. Shrainman, and H. Sompolinsky, Phys. Rev. A **45**, 3516 (1992).

[2] D. Hansel, G. Mato, and C. Meunier, Phys. Rev. E **48**, 3470 (1993).

[3] R. FitzHugh, Biophys. J. **1**, 445 (1961).

[4] J. Rinzel, in *Nonlinear Diffusion*, edited by W. E. Fitzgibbon and H. F. Walker (Pitman, London, 1977).

[5] J. Nagumo, S. Arimoto, and S. Yoshizawa, Proc. IRE **50**, 2061 (1962).

[6] S. Kim, S. G. Lee, H. Kook, and J. H. Shin, in *Neural Networks: The Statistical Mechanics Perspective*, edited by J. H. Oh, C. Kwon, and S. Cho (World Scientific, Singapore, 1995), pp. 141–155.

[7] S. G. Lee, S. Kim, and H. Kook, Int. J. Bifurcation Chaos Appl. Sci. Eng. **7**, 889 (1997).

[8] S. Kim, H. Kook, S. G. Lee, and M. H. Park, Int. J. Bifurcation Chaos Appl. Sci. Eng. **8**, 731 (1998).

[9] E. R. Kandel, J. H. Schwartz, and T. M. Jessel, in *Principles of Neural Science*, 3rd ed., edited by E. R. Kandel, J. H. Schwartz, and T. M. Jessel (Appleton & Lange, Norwalk, 1991), Chap. 9.

[10] T. Yoshinaga, Y. Sano, and H. Kawakami, Int. J. Bifurcation Chaos Appl. Sci. Eng. **9**, 1451 (1999).

[11] A. L. Hodgkin and A. F. Huxley, J. Physiol. (London) **117**, 500 (1952).

[12] K. Tsumoto, T. Yoshinaga, and H. Kawakami, Int. J. Bifurcation Chaos Appl. Sci. Eng. **11**, 1053 (2001).

[13] K. Ikeda, K. Otsuka, and K. Matsumoto, Prog. Theor. Phys. Suppl. **99**, 295 (1989).

[14] K. Kaneko, Physica D **41**, 137 (1990).

[15] I. Tsuda, E. Koerner, and H. Shimizu, Prog. Theor. Phys. **78**, 51 (1987).

[16] K. Nakano, IEEE Trans. Syst. Man Cybern. **SMC-2(3)**, 381 (1972).

[17] T. Kohonen, IEEE Trans. Comput. **C-21(4)**, 353 (1972).

[18] H. Kawakami, IEEE Trans. Circuits Syst. **CAS-31**, 246 (1984).

[19] M. Golubitsky and D. Schaeffer, *Singularities and Groups in Bifurcation Theory* (Springer, New York, 1985), Vol. I.

[20] M. Golubitsky, I. Stewart, and D. Schaeffer, *Singularities and Groups in Bifurcation Theory* (Springer, New York, 1985), Vol. II.